Turing instability in oscillator chains with nonlocal coupling

R. L. Viana,* F. A. dos S. Silva, and S. R. Lopes
Departamento de Física, Universidade Federal do Paraná, Caixa Postal 19044, 81531-990, Curitiba, Paraná, Brazil
(Received 20 September 2010; published 25 April 2011)

We investigate analytically and numerically the conditions for the Turing instability to occur in a one-dimensional chain of nonlinear oscillators coupled nonlocally, in such a way that the coupling strength decreases with the spatial distance as a power law. A range parameter makes it possible to cover the two limiting cases of local (nearest-neighbor) and global (all-to-all) couplings. We consider an example from a nonlinear autocatalytic reaction-diffusion model.

DOI: 10.1103/PhysRevE.83.046220 PACS number(s): 89.75.Kd, 47.54.Bd, 82.40.Ck

I. INTRODUCTION

Given the diversity of spatial patterns observed in nature, it is always puzzling to wonder how this diversity arises from spatially uniform situations. This question was pursued in the 1950s by Turing in his seminal paper on the mechanism of morphogenesis [1], in which he considered how a spatially homogeneous state can lose stability, giving rise to a spatially nonhomogeneous pattern, the so-called Turing instability. Turing analyzed a reaction-diffusion system comprised of spatially coupled ordinary differential equations that modeled discrete biological cells.

Turing put forward two basic assumptions: (i) the need for at least two chemical substances (morphogenes), an activator and an inhibitor, and (ii) diffusion plays a destabilizing role in the interacting chemical substances. The latter point is somewhat counterintuitive because diffusion usually smooths out spatial structures in linear systems and thus would be expected to exert a stabilizing influence instead. Moreover, Turing found that the instability caused by diffusion leads to the growth of spatial structures at a particular wavelength. This mechanism has successfully explained a wealth of pattern formation phenomena in nature, such as the segmentation patterns in the developing fly embryo, the periodic array of tentacles around the mouth of the hydra, zebra stripes [2], and seashell striations [3], to name just a few. In physical chemistry, the Turing instability has been found in many continuously fed stirred-tank reactors, as in the reaction of chlorine dioxide with iodine and malonic acid [4,5].

From the mathematical point of view, the Turing instability arises when an otherwise stable homogeneous state becomes unstable as a result of diffusion, in the sense that any small perturbation will develop into a spatially nonuniform state. Linear theory can predict the wavelength of the unstable mode that grows [6]. This growth, however, is limited by the saturating effect of nonlinear terms and a spatially nonhomogeneous pattern is then formed as a result of the Turing instability.

The Turing instability is usually investigated in the context of local couplings, in which each cell interacts with its nearest neighbors only. This is modeled by Fick's law, which states that the diffusive flux of morphogenes (activator and inhibitor) is proportional to their local concentration and is responsible for the second spatial derivatives in the mathematical models of such reaction-diffusion systems. However, there are many situations in which this picture is oversimplified, as in chemical couplings between biological cells that generate nonlocal interactions that cannot be described by a diffusive coupling. Nonlocal couplings can be implemented in macroscopic density equations in which the diffusion coefficient depends on a weighted spatial average of the density [7].

Such nonlocal couplings take into account not only the nearest neighbors of a given cell, but also the other cells of the assembly. An extreme form of this arises when each cell couples with the mean field produced by all the other cells, the so-called global (all-to-all) coupling, which is used in models of neural networks [8], coupled Josephson junctions [9], and is the basis of the paradigmatic Kuramoto model [10]. It is possible to interpolate between nearest-neighbor and all-to-all couplings by considering an interaction term whose strength decreases with the physical distance between cells as a power law [11]. This model has been used in theoretical and numerical studies of various spatiotemporal phenomena such as synchronization, shadowing, and cluster formation [12].

The influence of nonlocal couplings on the formation of Turing patterns has been studied in many systems. The conditions for the occurrence of the Turing instability were investigated for logistic growth processes using various nonlocal coupling terms [13]. In another recent study, a three-variable Oregonator model of a light-sensitive Belousov-Zhabotinsky reaction was studied, in which the nonlocal coupling was externally imposed by an optical feedback loop [14]. In the latter investigation, it was found that long-range inhibition leads to the Turing instability, whereas long-range activation induces wavelike patterns.

This work aims to investigate the presence of Turing instabilities in oscillator chains with a nonlocal coupling of the power-law form in order to have results that hold for both local and global cases. We derive analytically the conditions for a Turing instability to occur in a one-dimensional lattice of two-dimensional systems (representing the activator-inhibitor pair) undergoing linear dynamics. Then we study a nonlinear reaction-diffusion system proposed by Meinhardt and Gierer [15] as a model for pattern formation related to skin pigmentation.

The rest of this paper is organized as follows. In Sec. II we introduce the oscillator model to be studied, as well as the type of coupling between the units. The analytical conditions

*viana@fisica.ufpr.br

for a Turing instability to occur are derived in Sec. III using linear stability theory. The effect of nonlinear terms and the ensuing pattern formation is discussed in Sec. IV through the Meinhardt-Gierer model. Our conclusions are given in Sec. V.

II. OSCILLATOR CHAIN WITH NONLOCAL COUPLING

Let us consider an oscillator one-dimensional chain with N units, each of them being a nonlinear reaction-diffusion system, whose dynamical state is described by the concentrations of the activator $x_k(t)$ and inhibitor $y_k(t)$, satisfying the following equations ($k = 1,2,\ldots,N$):

$$\dot{x}_k = \mathbf{X}(x_k,y_k) - D_x x_k + \frac{D_x}{\kappa(\alpha)} \sum_{r=1}^{N'} \frac{1}{r^\alpha}(x_{k-r} + x_{k+r}), \quad (1)$$

$$\dot{y}_k = \mathbf{Y}(x_k,y_k) - D_y y_k + \frac{D_y}{\kappa(\alpha)} \sum_{r=1}^{N'} \frac{1}{r^\alpha}(y_{k-r} + y_{k+r}), \quad (2)$$

where $\mathbf{X}$ and $\mathbf{Y}$ stand for the vector field corresponding to the uncoupled oscillators. We use a nonlocal form of coupling for which the interaction strength decreases with the lattice distance in a power-law fashion, where D_x and D_y are positive coupling constants representing the different diffusion coefficients of the chemical species, α is a positive real number, and

$$\kappa(\alpha) = 2\sum_{r=1}^{N'} \frac{1}{r^\alpha} \quad (3)$$

is a normalization factor, with $N' = (N-1)/2$, supposing that N is an odd number. In the oscillator chain given by Eqs. (1) and (2), the summation terms are weighted averages of discretized second spatial derivatives, the common normalization factor $\kappa(\alpha)$ being the sum of the corresponding weights.

In the limit $\alpha \to \infty$, only the $r = 1$ term will survive in the summation terms, resulting in $\kappa \to 2$ and the Laplacian or diffusive coupling,

$$\dot{x}_k = \mathbf{X}(x_k,y_k) + \frac{D_x}{2}(x_{k-1} - 2x_k + x_{k+1}), \quad (4)$$

$$\dot{y}_k = \mathbf{Y}(x_k,y_k) + \frac{D_y}{2}(y_{k-1} - 2y_k + y_{k+1}), \quad (5)$$

in which only the nearest neighbors of a given site contribute to the coupling term. The other limiting case, $\alpha = 0$, is such that $\kappa(0) = N - 1$ and the oscillator chain becomes globally coupled,

$$\dot{x}_k = \mathbf{X}(x_k,y_k) + D_x\left(-x_k + \frac{1}{N-1}\sum_{r=1,r\neq k}^{N} x_r\right), \quad (6)$$

$$\dot{y}_k = \mathbf{Y}(x_k,y_k) + D_y\left(-y_k + \frac{1}{N-1}\sum_{r=1,r\neq k}^{N} y_r\right), \quad (7)$$

where each oscillator interacts with the mean value of all lattice sites, irrespective of their positions (mean-field model). Hence, the coupling term in Eqs. (1) and (2) may be regarded as an interpolating form between these limiting cases and will be referred to as a power-law coupling.

III. LINEAR STABILITY

Let us consider the equilibrium values of the activator and inhibitor given by X_0 and Y_0, respectively. The deviations from these values (also denoted by x and y, for notational simplicity), in lowest order, obey a linearized model for which the activator-inhibitor dynamics in each uncoupled oscillator (labeled by k, as before) are governed by the affine vector field

$$\mathbf{X}(x_k,y_k) = ax_k + by_k, \quad (8)$$

$$\mathbf{Y}(x_k,y_k) = cx_k + dy_k, \quad (9)$$

where the constants a,b,c,d are the elements of the Jacobian matrix of the nonlinear vector field evaluated at (X_0,Y_0). The equilibrium solution of the linearized system is $(x^* = 0, y^* = 0)$, which is linearly stable if

$$q \equiv ad - bc > 0, \qquad a + d < 0. \quad (10)$$

The convergence to the equilibrium will be monotonic if $(a-d)^2 + 4bc > 0$ and oscillatory if this factor is negative. This set of conditions shall be supposed from now on.

In order to treat the coupled system, we can use a discrete Fourier transform of each dynamical variable, in the following form:

$$x_k(t) = \sum_{s=0}^{N-1} \xi_s(s,t)\exp\left(\frac{2\pi isk}{N}\right), \quad (11)$$

$$y_k(t) = \sum_{s=0}^{N-1} \eta_s(s,t)\exp\left(\frac{2\pi isk}{N}\right), \quad (12)$$

where ξ_s and η_s are time-dependent Fourier-mode amplitudes. On substituting Eqs. (11) and (12) in the linearized version of Eqs. (1) and (2) we find that the mode amplitudes satisfy uncoupled linear differential equations

$$\dot{\xi}_s = [a - 2D_x\sigma_\alpha(s,N)]\xi_s + b\eta_s = a_\sigma\xi_s + b\eta_s, \quad (13)$$

$$\dot{\eta}_s = [d - 2D_y\sigma_\alpha(s,N)]\xi_s + c\eta_s = c\xi_s + d_\sigma\eta_s, \quad (14)$$

where we define the auxiliary quantities

$$a_\sigma \equiv a - 2D_x\sigma_\alpha(s,N), \quad (15)$$

$$d_\sigma \equiv d - 2D_y\sigma_\alpha(s,N), \quad (16)$$

where

$$\sigma_\alpha(s,N) \equiv \frac{1}{2} - \frac{1}{\kappa(\alpha)}\sum_{r=1}^{N'} \frac{1}{r^\alpha}\cos\left(\frac{2\pi sr}{N}\right) \quad (17)$$

is a function whose values are such that $0 \leqslant \sigma_\alpha(s,N) \leqslant \sigma_{\max}(\alpha,N) \leqslant 1$ (Fig. 1). For the nearest-neighbor case ($\alpha \to \infty$) it turns out that

$$\sigma_\infty(s,N) = \sin^2\left(\frac{\pi s}{N}\right), \quad (18)$$

for which $\sigma_{\max} = 1$ reaches its largest value [Fig. 1(b)]. In contrast, in the mean-field coupling ($\alpha = 0$) this function reads

$$\sigma_0(s,N) = \frac{1}{2}\left(\frac{N}{N-1}\right)(1 - \delta_{s,0}), \quad (19)$$

such that for large N it tends to $1/2$ [Fig. 1(a)].

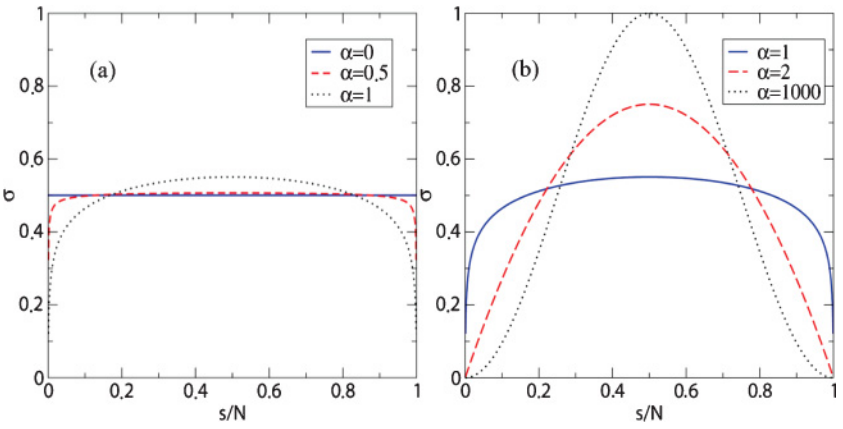

FIG. 1. (Color online) Dependence of the function defined by Eq. (17) on the argument s/N, for (a) small and (b) large values of the parameter α.

The Turing instability occurs when a spatially homogeneous pattern becomes inhomogeneous by virtue of the coupling effect, which acts as a perturbation on each oscillator, driving it out of its equilibrium state. The equilibrium point of the linearized mode amplitude equations, $(\xi_s,\eta_s) = (0,0)$, corresponds to equilibrium concentrations of activator and inhibitor species for each oscillator. Hence the onset of a Turing instability happens whenever this equilibrium becomes an unstable saddle point, which occurs if

$$q_\sigma \equiv a_\sigma d_\sigma - bc = 4D_xD_y\sigma^2 - 2\sigma(aD_y - dD_x) + q < 0. \tag{20}$$

On defining the auxiliary variables

$$P \equiv \frac{a}{D_x} + \frac{d}{D_y}, \qquad Q \equiv \frac{ad-bc}{D_xD_y}, \tag{21}$$

the inequality in Eq. (20) is satisfied provided $\sigma_- < \sigma < \sigma_+$, where

$$\sigma_\pm \equiv \frac{P \pm \sqrt{P^2-4Q}}{4}. \tag{22}$$

Since the function σ has the upper bound $\sigma_{\max}(\alpha,N) \leqslant 1$ we must have $0 \leqslant \sigma_- \leqslant \sigma_{\max}(\alpha,N)$, such that $0 \leqslant P - \sqrt{P^2-4Q} \leqslant 4\sigma_{\max}(\alpha,N)$, which gives the following conditions for the appearance of the Turing instability in the system:

$$Q > 0, \tag{23}$$

$$P > 2\sqrt{Q} \quad \text{if} \quad 0 \leqslant P \leqslant 4\sigma_{\max}(\alpha,N), \tag{24}$$

$$P > \frac{Q}{2\sigma_{\max}(\alpha,N)} + 2\sigma_{\max}(\alpha,N) \ \text{ if } \ P > 4\sigma_{\max}(\alpha,N). \tag{25}$$

Hence the stability of the spatially homogeneous state in this system depends on the values taken on by $\sigma_{\max}$. In Fig. 2, we show how this stability depends on the range parameter α by direct numerical evaluation of the function extremum (solid curve) and using an analytical approximation (dashed curve). The latter was obtained as follows. First, we can show from Eq. (17) that this function is always symmetric with respect to $s = N/2$,

$$\sigma_\alpha(s = N/2 + L,N) = \sigma_\alpha(s = N/2 - L,N)$$

for all L values such that $0 \leqslant s \leqslant N-1$. By the same token we show that $\sigma_\alpha(s,N)$ has a local maximum at $s = N/2$ (for $N' = (N-1)/2$ odd)

$$\left.\frac{\partial\sigma_\alpha(s,N)}{\partial s}\right|_{s=N/2} = 0, \qquad \left.\frac{\partial^2\sigma_\alpha(s,N)}{\partial s^2}\right|_{s=N/2} < 0,$$

such that

$$\sigma_{\max}(\alpha,N) = \sigma_\alpha(s = N/2,N).$$

Finally, if N is large enough that s/N can be reasonably well approximated by a continuous variable, we can use the Euler-MacLaurin formula [16] to replace the summation in (17) by an integral, which yields an analytical approximation for $\sigma_{\max}$,

$$\begin{aligned}\sigma_{\max}(\alpha,N) \approx{}& \frac{1}{2} - \frac{1}{2}\left(\frac{1-(N')^{1-\alpha}}{\alpha-1} + \frac{N'^{-\alpha}+1}{2}\right)^{-1} \\ &\times\left\{\left[-\frac{1}{2}\left(\frac{1-(N')^{1-\alpha}}{\alpha-1}\right) - \left(\frac{N'^{-\alpha}+1}{2}\right)\right]\right. \\ &+\left[\frac{2^{-\alpha}}{\alpha-1}(1-2^{\alpha-1}(N'-1)^{1-\alpha})\right. \\ &\left.\left.+\frac{(N'-1)^{-\alpha}+2^{-\alpha}}{2}\right]\right\},\end{aligned} \tag{26}$$

which holds for odd values of N'. We see that the approximation always underestimates the actual value of $\sigma_{\max}(\alpha,N)$, but the difference turns out not to be large, especially at small α. In contrast, for large α, while the analytical approximation gives worse results, we already know that this value must approach unity since this is the nearest-neighbor coupling case. Notice that the large-N limit has to be taken only as an approximation for obtention of closed-form analytical expressions. In fact, for $N \to \infty$ the power-law coupling in Eqs. (1) and (2) is not normalizable when $0 < \alpha < 1$ [17].

In the case of the local (nearest-neighbor) coupling ($\alpha \to \infty$) we have large values of α and $\sigma_{\max}$ tends to unity, such that the conditions in Eqs. (23) and (25) for a Turing instability to occur reduce to

$$Q > 0, \tag{27}$$

$$P > 2\sqrt{Q} \quad \text{if} \quad 0 \leqslant P \leqslant 4, \tag{28}$$

$$P > \frac{Q}{2} + 2 \quad \text{if} \quad P > 4, \tag{29}$$

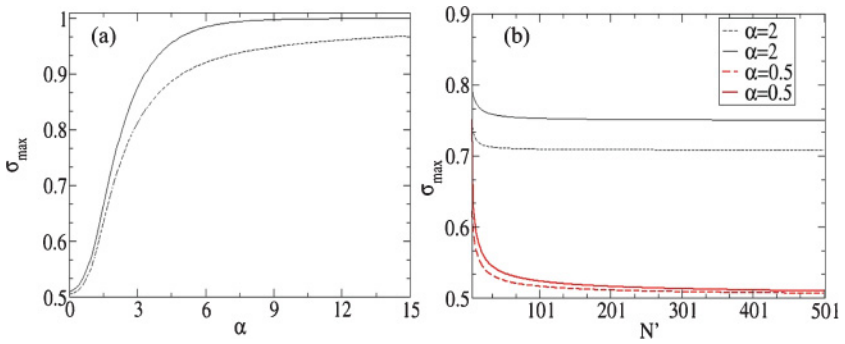

FIG. 2. (Color online) Dependence of the maximum value of $\sigma_\alpha(s,N)$ on the parameters (a) α and (b) N. In both figures, the solid curves represent numerical evaluations, whereas the dashed curves result from analytical approximations.

which agrees with the results of Ref. [6] up to a (nonessential) factor of 2 due to a slightly different definition of the local coupling prescription.

Since the uncoupled oscillators are supposed to have a stable equilibrium concentration, the local conditions in Eq. (10) apply, such that Eq. (27) always holds. The remaining conditions depend on the values of the diffusion coefficients. It is instructive to consider the case where both diffusion coefficients are equal, $D_x = D_y = D$. In this case it turns out that $P = (a+d)/D$ is negative and a Turing instability cannot occur. In fact, it is well known that pattern formation in a chemical system will not occur unless the diffusion coefficients of the activator and inhibitor differ substantially [5].

The range of unstable modes in the local coupling case is given by

$$\min(\sigma_+,1) > \sigma > \sigma_-, \tag{30}$$

where $\sigma_\pm$ are given by Eq. (22). Notice that we have $\sigma_+ > 1$ provided $P < (Q/2) + 2$. Substituting Eq. (18) and solving the resulting inequalities, there result two intervals of unstable modes symmetrically located with respect to $s/N = 1/2$,

$$\begin{aligned} \frac{\sin^{-1}\sqrt{\sigma_-}}{\pi} < \frac{s}{N} < \frac{\sin^{-1}\sqrt{\sigma_+}}{\pi}, \\ 1 - \frac{\sin^{-1}\sqrt{\sigma_+}}{\pi} < \frac{s}{N} < 1 - \frac{\sin^{-1}\sqrt{\sigma_-}}{\pi}. \end{aligned} \tag{31}$$

In this way, a larger number of modes become unstable if $\sigma_+ > 1$.

The global (all-to-all) case ($\alpha = 0$) presents interesting features as the function $\sigma_0(s,N)$ takes on a constant value σ_0 given by Eq. (19). The conditions in Eqs. (23) and (25) hence reduce to a single inequality

$$P > \frac{Q}{2\sigma_0} + 2\sigma_0, \tag{32}$$

in such a way that once this condition is fulfilled all modes become simultaneously unstable. Since for large N we have $\sigma_0 \approx 1/2$, the relation above can be written in a simple form, $P > Q + 1$. It is interesting to note that if the diffusion coefficients are equal this condition cannot be satisfied in general, as in the local case. Thus, there is a range-independent influence of the dissimilarity of the diffusion coefficients on the occurrence of a Turing instability.

Let us consider a specific example of the intermediate range case for which $\alpha = 1$ and we take a chain with $N = 101$ oscillators. Then Eq. (17) gives $\sigma_{\max} \approx 0.577$ for this case. The approximation expressed by Eq. (26), which works well also for N' even, would give a slightly smaller value of 0.568 for $\sigma_{\max}$. On substituting the value of $\sigma_{\max}$ in Eqs. (23) and (25) we obtain conditions for the existence of a Turing instability that can be better represented in the parameter plane depicted (for α arbitrary) in Fig. 3(a) where we draw the lines where there is marginal stability as a function of parameters P and Q. Since for $\alpha = 1$ the function σ has a broad flat top, failing on being a constant (as in the global case) only for the vicinity of the extremities $s/N = 0$ and 1, we have roughly the same behavior in that most modes become unstable simultaneously in the intermediate-range case.

The stable area $A_{\rm st}$, or the area in the parameter plane for which we have stable equilibria, provides useful information. In Fig. 3(b) we show a magnification of a region of large-Q values in the parameter plane for different values of α. It is apparent that the stable area decreases with increasing α (i.e., the relative number of parameter values yielding stable equilibria becomes larger as the coupling becomes global and smaller as the coupling becomes local). By integrating out the stability curves in Fig. 3(a), from $Q = 0$ to an arbitrary Q_0, it is actually possible to derive an analytical expression for the stable area (normalized by Q_0^2), which reads

$$A_{\rm st} = \frac{1}{4\sigma_{\max}} + \frac{\sigma_{\max}(2Q_0 - 4)}{Q_0^2} + \frac{32\sigma_{\max}^{3/2}}{3Q_0^2} - 8\frac{\sigma_{\max}^2}{Q_0^2}, \tag{33}$$

giving, for large Q_0, $A_{\rm st} \approx 1/4\sigma_{\max}$. In very long oscillator chains where N is large with local and global couplings, $\sigma_{\max}$ takes on values equal to 1 and 1/2, respectively. Hence the stable area in the local case is roughly half of the corresponding area in the global case. We thus conclude that a Turing instability would be statistically more common for local couplings than for global ones.

IV. NONLINEAR REACTION-DIFFUSION MODEL

In reaction-diffusion systems of practical interest there are nonlinear terms that exert saturation on the nonhomogeneous spatial modes excited by the Turing instability, giving rise to pattern formation. The basic mechanism of this saturation combines a short-range autocatalytic activation, which causes self-enhancement after a Turing instability sets in, with a long-range inhibitory effect. The latter can be caused by either a rapidly spreading and long-range (or a result from a) depletion of material required for the self-enhancement that is obtained from the surrounding region [15].

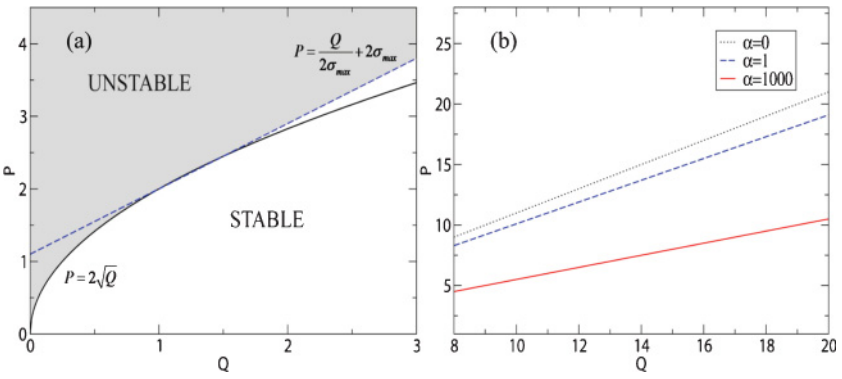

FIG. 3. (Color online) (a) Parameter plane showing the lines of marginal stability for the case of $N = 101$ coupled oscillators and arbitrary α. (b) Magnification of a region of (a) of large-Q values.

A paradigm of this broad class of reaction-diffusion systems is the Meinhardt-Gierer model, which, in the language of Eqs. (1) and (2), reads [15,18]

$$\mathbf{X}(x_k, y_k) = \rho_x \frac{x_k^2}{y_k} - \mu_x x_k, \tag{34}$$

$$\mathbf{Y}(x_k, y_k) = \rho_y x_k^2 - \mu_y y_k, \tag{35}$$

where $\rho_{x,y}$ and $\mu_{x,y}$ are positive parameters characterizing the local reaction rates. The term proportional to ρ_x comes from the assumption that the activator is an autocatalytic chemical species, its denominator representing the inhibitor effect of the other species. In this case ρ_x turns out to be a small activator-independent production rate of the activator and is actually necessary to start the activator autocatalysis at very low activator concentration, as in the case of regeneration. Likewise, ρ_y stands for a baseline production rate of the inhibitor [15]. The quantities μ_x and μ_y play the role of degradation of the activator and inhibitor species, respectively, such that the number of molecules of each species that decay per time unit is proportional to the corresponding decay rate and to the number of molecules themselves [19].

A. Stability analysis

We first determine the equilibrium points of the uncoupled vector field in Eqs. (34) and (35). One of them is obviously $x^* = y^* = 0$, whereas there is a nontrivial equilibrium with activator and inhibitor concentrations given, respectively, by

$$x^* = \frac{\rho_x \mu_y}{\rho_y \mu_x}, \qquad y^* = \frac{\rho_x^2 \mu_y}{\rho_y \mu_x^2}. \tag{36}$$

The linearized dynamics around this equilibrium, for the uncoupled case, is obtained from the Jacobian matrix of Eqs. (34) and (35), with elements evaluated at the point (x^*, y^*), giving the matrix elements

$$a = \mu_x, \qquad b = -\frac{\mu_x^2}{\rho_x}, \tag{37}$$

$$c = \frac{2\rho_x \mu_y}{\mu_x}, \qquad d = -\mu_y. \tag{38}$$

If the equilibrium (x^*, y^*) is to be stable, the trace and determinant of this Jacobian must be, respectively, negative and positive, yielding the conditions

$$\mu_x < \mu_y, \qquad \mu_x \mu_y > 0. \tag{39}$$

Since all coefficients are taken to be positive, this implies that the decay rate of the inhibitor must be greater than that of the activator, which is a reasonable assumption for having a stable equilibrium concentration of both species. The approach to the equilibrium is determined by the nature (real or complex) of the eigenvalues of the Jacobian. The results of this simple analysis are summarized in Fig. 4. Similarly, the equilibrium at the origin can be shown to be always unstable and thus it is not relevant when discussing Turing instability due to diffusion.

Now we turn into the coupled system in Eqs. (1) and (2), for which there is a spatially homogeneous equilibrium state given by

$$x_k = x^*, \qquad y_k = y^*. \qquad (k = 1,2,\ldots,N) \tag{40}$$

This state defines a two-dimensional invariant subspace embedded into the full $2N$-dimensional phase space of the coupled oscillator chain. The subspace is invariant because any trajectory that originates from an initial condition belonging to this subspace is bound to lie within it for further times. Geometrically speaking, the possible spatially nonhomogeneous states one may find represent trajectories outside this invariant subspace.

In this geometrical language, we are interested in investigating the stability of the invariant homogeneous subspace along the $2(N-1)$ remaining transversal directions. We can

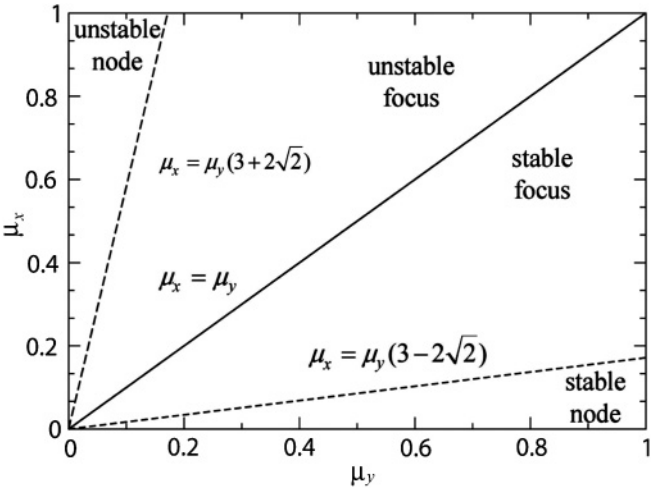

FIG. 4. Stability of the uncoupled equilibrium points of the Meinhardt-Gierer equations in the parameter plane μ_x vs μ_y.

use the results of Sec. II to obtain analytical conditions for the stability of the spatially homogeneous state. The substitution of Eqs. (37) and (38) into Eq. (21) results in the stability conditions in Eqs. (23) and (25), which read

$$\frac{\mu_x \mu_y}{D_x D_y} > 0, \tag{41}$$

$$\begin{aligned} &\mu_x D_y - \mu_y D_x > 2\sqrt{\mu_x \mu_y D_x D_y} \\ \text{if} \quad &0 \leqslant \mu_x D_y - \mu_y D_x \leqslant 4\sigma_{\max} D_x D_y, \end{aligned} \tag{42}$$

$$\begin{aligned} &\mu_x D_y - \mu_y D_x > \frac{\mu_x \mu_y}{2\sigma_{\max}} + 2\sigma_{\max} D_x D_y \\ \text{if} \quad &\mu_x D_y - \mu_y D_x > 4\sigma_{\max} D_x D_y. \end{aligned} \tag{43}$$

Since the uncoupled oscillators are supposed to be locally stable so that Eq. (39) holds, the condition in Eq. (41) is always fulfilled, as the diffusion coefficients are positive-definite.

Let us consider the limit cases of this coupling. For the nearest-neighbor case (large α) we have $\sigma_{\max} = 1$. If the diffusion coefficients were equal, there would be no Turing instability, as shown before. For the all-to-all coupling ($\alpha = 0$) the conditions in Eqs. (42) and (43) reduce to the single inequality (valid for large N):

$$\mu_x D_y - \mu_y D_x > \mu_x \mu_y + D_x D_y. \tag{44}$$

The threshold for the Turing instability is depicted in the parameter plane D_x vs D_y (for fixed values of the remaining parameters) (Fig. 5).

B. Pattern formation

In the numerical simulations to be presented, we use a predictor-corrector routine (LSODA) based on the Adams method [20] and the same values for the parameters of the Meinhardt-Gierer model as those chosen in Ref. [21]: $\mu_x = 0.01$, $\mu_y = 0.02$, $\rho_x = 0.01$, and $\rho_y = 0.02$, for which the equilibrium point is a stable focus with coordinates $(x^*, y^*) = (1.0, 1.0)$. We also fix the diffusion coefficient of the inhibitor at $D_y = 0.2$ and use the activator coefficient D_x as the tunable parameter for each value chosen for the effective range α. We use, as an initial condition, an almost homogeneous spatial profile with a tiny bump that is intended to be a seed for some unstable mode to grow after a Turing instability occurs.

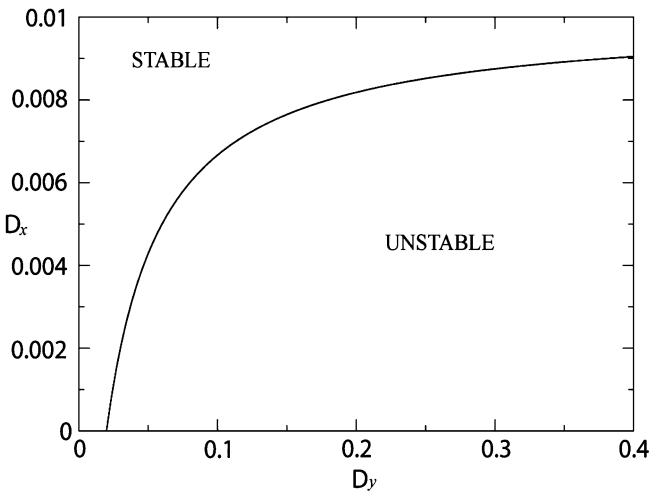

FIG. 5. Parameter plane of the activator and inhibitor diffusion coefficients for $\mu_x = 0.01$, $\mu_y = 0.02$, $\rho_x = 0.01$, and $\rho_y = 0.02$.

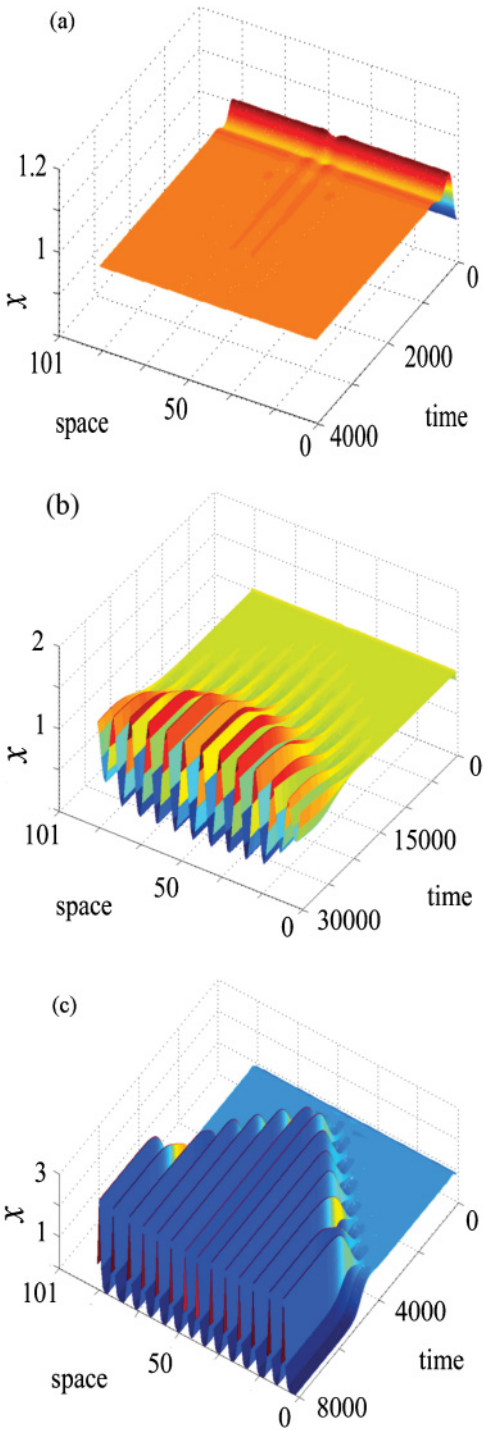

FIG. 6. (Color online) Space-time diagrams of the activator concentration for the nearest-neighbor coupling case, $D_x = 0.2$, and (a) $D_y = 0.019$, (b) $D_y = 0.016$, and (c) $D_y = 0.005$.

The local case (large α) is illustrated by Fig. 6, where we depict space-time diagrams (activator concentration x versus discrete space k and time t) for different values of

the activator diffusion coefficient. For relatively large D_x [Fig. 6(a)] we do not observe pattern formation, since we are above the instability threshold predicted by the linear theory. The oscillators go together to the homogeneous equilibrium state $x^* = 1$ instead. The instability threshold occurs for $D_x \approx 0.016$ and we accordingly observe the emergence of a spatially nonhomogeneous pattern just after the Turing instability [Fig. 6(b)].

This pattern is roughly a sinusoidal spatial profile with 12 maxima, corresponding to a wavelength of $\lambda \approx 8.42$ and thus to a wave number

$$\frac{s}{N} = \frac{1}{\lambda} \approx 0.119.$$

From the linear stability analysis, the parameter set used to generate Fig. 6(b) corresponds to $\sigma_- = 0.09$ and $\sigma_+ = 0.17$. Using Eq. (31), the ranges of unstable modes are [0.097,0.135] and [0.865,0.903]. The pattern observed has a wave number roughly in the middle of the interval of unstable modes (i.e., it is the most unstable mode from the linear approximation).

As we substantially decrease the activator diffusion coefficient, we observe another spatial pattern [Fig. 6(c)] with 14 maxima and thus a smaller wavelength than the previous example, namely

$$\frac{s}{N} = \frac{1}{7.21} \approx 0.139,$$

which belongs again to one of the intervals of linearly unstable modes, [0.076,0.392] and [0.608,0.924]. It is no longer the most unstable mode, however. A larger wave number such as this is actually a general feature of spatiotemporal systems when we decrease the diffusion coefficient—modes with small wave numbers are more easily damped when diffusion increases, as a general rule.

The corresponding space-time plots for the global (all-to-all) coupling case are shown in Figs. 7(a) and 7(b) for parameters before and after the occurrence of a Turing instability, respectively. According to the linear theory (see Fig. 5) it occurs for $D_x \approx 0.008$. The pattern formed after the Turing instability is more complex than in the previous example and cannot be assigned to a single unstable mode, but rather to an entire spectrum of unstable modes excited by the Turing instability, which became stabilized by the saturating effect of the nonlinear terms of the model, a feature obviously not present in the linear stability analysis of Sec. V A. The space-time plots for the intermediate-range

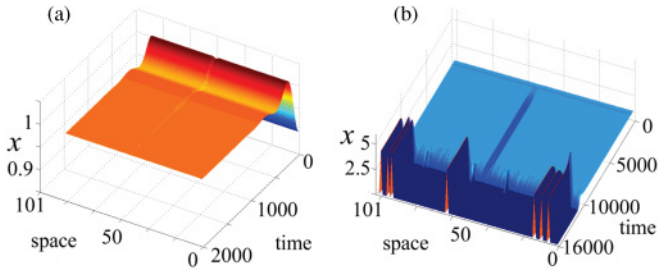

FIG. 7. (Color online) Space-time diagrams of the activator concentration for the all-to-all (global) coupling case, $D_x = 0.2$, and (a) $D_y = 0.009$ and (b) $D_y = 0.005$.

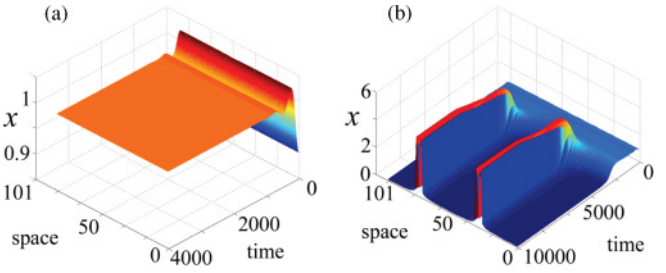

FIG. 8. (Color online) Space-time diagrams of the activator concentration for the intermediate-range coupling of $\alpha = 1.0$, $D_x = 0.2$, (a) $D_y = 0.020$, and (b) $D_y = 0.005$.

coupling characterized by $\alpha = 1.0$ are depicted in Figs. 8(a) and 8(b), before and after the threshold of a Turing instability, respectively.

V. CONCLUSIONS

The Turing instability is a general mechanism of pattern formation from which a spatially homogeneous pattern becomes unstable and develops a spatial structure after saturation that comes from nonlinear effects. In biological scenarios there may be the need for nonlocal couplings, or interactions among distant cells, not only the nearest neighbors, as in typical studies of spatial diffusion. We have presented an analytical study of the occurrence of the Turing instability in coupled oscillator chains with nonlocal interactions. We presented a linear stability analysis for the Turing instability when the coupling among sites is nonlocal (i.e., it takes into account not only the nearest neighbors but also all the other oscillators in a one-dimensional chain) the coupling strength decreasing with the lattice distance as a power law.

We have shown, using a specific nonlinear model, that the linear stability analysis is useful to characterize the Turing instability when nonlocal couplings are considered. In particular, we derived analytical conditions for the presence of Turing instability for an arbitrary effective coupling range. Our results agree, in the short-range limit, with results obtained for nearest-neighbor couplings and can be also applied to situations with global (all-to-all) couplings. We have shown that local couplings have a comparatively shorter stable area in the parameter plane than global couplings. In other words, as the effective coupling range increases, the more stable the spatial configurations become and, statistically speaking, the less probable the occurrence of a Turing instability would be.

This can be qualitatively understood by noting that global couplings spread information among cells more rapidly than local couplings, for which diffusion happens at a slower rate. Then globally coupled cells are less likely to present a Turing instability than locally coupled cells. In contrast, other dynamical collective phenomena due to interactions, such as frequency synchronization [22], short-term memory formation [23], and bursting synchronization [24], are more likely to occur in the globally than locally coupled chains.

The question of pattern formation, however, is more complex since the patterns are ultimately determined by

nonlinear features of the model that are not predictable by linear stability analysis. Even so, in some cases it is possible to relate single-mode patterns to the modes that become unstable after a Turing instability.

ACKNOWLEDGMENTS

This work was made possible in part by financial support from CNPq, CAPES, Fundação Araucária, and RNF-CNEN (Brazilian Fusion Network).

[1] A. Turing, Philos. Trans. R. Soc. London Ser. B **237**, 37 (1952).
[2] J. D. Murray, *Mathematical Biology*, 2nd ed. (Springer, Berlin, 1993).
[3] H. Meinhardt and M. Klingler, J. Theor. Biol. **126**, 63 (1987).
[4] I. Lengyel, G. Rábai, and I. Epstein, J. Am. Chem. Soc. **112**, 4606 (1990).
[5] S. Setayeshgar and M. C. Cross, Phys. Rev. E **58**, 4485 (1998); **59**, 4258 (1999).
[6] E. Atlee-Jackson, *Perspectives in Nonlinear Dynamics* (Cambridge University Press, Cambridge, 1991), Vol. II.
[7] C. Lopez, Phys. Rev. E **74**, 012102 (2006).
[8] M. G. Rosenblum and A. S. Pikovsky, Phys. Rev. Lett. **92**, 114102 (2004).
[9] K. Y. Tsang, R. E. Mirollo, S. H. Strogatz, and K. Wiesenfeld, Physica D **48**, 102 (1991).
[10] Y. Kuramoto, *Chemical Oscillations, Waves, and Turbulence* (Dover, New York, 2003).
[11] J. L. Rogers and L. T. Wille, Phys. Rev. E **54**, R2193 (1996).
[12] S. E. de S. Pinto, S. R. Lopes, and R. L. Viana, Physica A **303**, 339 (2002).
[13] N. M. Shnerb, Phys. Rev. E **69**, 061917 (2004).
[14] E. M. Nicola, M. Bar, and H. Engel, Phys. Rev. E **73**, 066225 (2006).
[15] H. Meinhardt, *Models of Biological Pattern Formation* (Academic, New York, 1992).
[16] P. B. Kahn, *Mathematical Methods for Scientists and Engineers* (Wiley, New York, 1990).
[17] G. Paladin and A. Vulpiani, J. Phys. A **25**, 4911 (1994); A. Torcini and S. Lepri, Phys. Rev. E **55**, R3805 (1997).
[18] A. Gierer and H. Meinhardt, Kybernetik **12**, 30 (1972).
[19] A. Gierer, Prog. Biophys. Mol. Biol. **37**, 1 (1981).
[20] A. C. Hindmarch, in *Scientific Computing*, IMACS Transactions on Scientific Computation, edited by R. S. Stepleman, M. Carver, R. Peskin, W. F. Ames, and R. Vichnevetsky, (North-Holland, Amsterdam, 1983), Vol. 1, p. 5564.
[21] H. Meinhardt and J. A. Koch, Rev. Mod. Phys. **66**, 1481 (1994).
[22] S. E. de S. Pinto and R. L. Viana, Phys. Rev. E **61**, 5154 (2000).
[23] J. C. A. de Pontes, A. M. Batista, R. L. Viana, and S. R. Lopes, Physica A **368**, 387 (2006).
[24] J. C. A. de Pontes, R. L. Viana, S. R. Lopes, C. A. S. Batista, and A. M. Batista, Physica A **387**, 4417 (2008).